Proceedings of Meetings on Acoustics

Volume 19, 2013 http://acousticalsociety.org/

ICA 2013 Montreal
Montreal, Canada
2 - 7 June 2013

Structural Acoustics and Vibration
Session 4aSA: Applications in Structural Acoustics and Vibration II

4aSA8. Sound generated by a wing with a flap interacting with an eddy

Avshalom Manela* and Lixi Huang

***Corresponding author's address: Technion, Haifa, 32000, N/A, Israel, avshalom@aerodyne.technion.ac.il**

Acoustic signature of a rigid wing, equipped with a movable downstream flap and interacting with a line vortex, is studied in a two-dimensional low-Mach number flow. The flap is attached to the airfoil via a torsion spring, and the coupled fluid-structure interaction problem is analysed using thin-airfoil methodology and application of the Brown and Michael equation. It is found that incident vortex passage above the airfoil excites flap motion at the system natural frequency, amplified above all other frequencies contained in the forcing vortex. Far-field radiation is analysed using Powell-Howe analogy, yielding the leading order dipole-type signature of the system. It is shown that direct flap motion has a negligible effect on total sound radiation. The characteristic acoustic signature of the system is dominated by vortex sound, consisting of relatively strong leading and trailing edge interactions of the airfoil with the incident vortex, together with late-time wake sound resulting from induced flap motion. In comparison with the counterpart rigid (non-flapped) configuration, it is found that the flap may act as sound amplifier or absorber, depending on the value of flap-fluid natural frequency. The study complements existing analyses examining sound radiation in static- and detached-flap configurations.

Published by the Acoustical Society of America through the American Institute of Physics

 [DOI: 10.1121/1.4799350]
Received 16 Jan 2013; published 2 Jun 2013

BACKGROUND AND PROBLEM FORMULATION

Airframe noise, and in particular sound generated by high-lift devices, is known to be a major cause for acoustic radiation, particularly during airplanes approach for landing [1]. Significant efforts have therefore been made to analyse the sound generated by such devices, in various setups and flight conditions. Common to almost all of these works is a *static* configuration of a *detached* lift device, where the acoustic field is affected mainly by vortex shedding and flow separation phenomena occurring at the gap between the airfoil and the flap [2]-[4]. Motivated by recent investigations of continuous “mold-line link" flap configurations [5], the objective of the present study is to consider an *attached*-flap configuration and examine the effect of flap *motion* on its acoustic radiation.

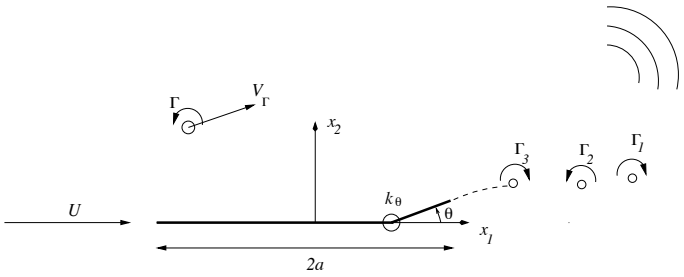

FIGURE 1: Schematic of the problem.

Schematic of the problem is given in Fig. 1. We consider a two-dimensional airfoil of chord $2a$ consisting of a stationary upstream part, aligned with the x_1-axis, and attached to a flap at $x_1 = \eta a$ (with $0 < \eta < 1$). The flap is hinged to the airfoil through a torsion spring of constant k_θ, and the system is subject to low-Mach high-Reynolds number flow of mean density ρ_0 and speed U in the x_1-direction. An incident line vortex of strength Γ is released into the flow at a given location, and moves past the airfoil-flap system. Fluid vorticity is assumed concentrated at the incident vortex location and along a trailing edge wake, with the latter discretized and modeled using the Brown and Michael equation [6, 7]. The near-field flow is treated by means of potential thin-airfoil methodology, while the far-field sound is analysed using Powell-Howe acoustic analogy [8].

To obtain a non-dimensional problem, the length, velocity, time and pressure are scaled by $a, U, a/U$ and $\rho_0 U^2$, respectively. The initial-value problem coupling between flap motion and near-field flow then consists of an angular equation of motion for the flap angle θ together with equations for the incident and trailing edge vortices dynamics. These are supplemented by a no-penetration condition on the airfoil, an unsteady Kutta condition ensuring finite fluid velocity at the trailing edge, and initial conditions specifying the system state at time $t = 0$. Omitting the presentation of full problem for brevity, we note the scaled form of the flap equation of motion for later reference,

$$\frac{\mathrm{d}^2\theta}{\mathrm{d}t^2} + \omega^2\theta = \beta \int_\eta^1 \Delta p(x_1, t)(x_1 - \eta)\mathrm{d}x_1, \tag{1}$$

where $\Delta p(x_1, t)$ marks the pressure jump across the airfoil owing to fluid loading, and is calculated via Bernoulli equation. Equation (1) is governed by the parameters

$$\eta\ ,\ \omega = \sqrt{\frac{k_\theta a^2}{I_f U^2}} \quad \text{and} \quad \beta = \frac{\rho_0 a^4}{I_f}, \tag{2}$$

with the latter two denoting the *system natural frequency* and *fluid-loading number*, respectively, and I_f marking the flap moment of inertia about its hinge. In addition, the problem

is governed by

$$\gamma = \frac{\Gamma}{2\pi a U} \quad \text{and} \quad \mathbf{x}_\gamma(0), \tag{3}$$

specifying the scaled incident vortex circulation and initial location, respectively. To illustrate our findings we focus on a case of an incident vortex with $\gamma = 0.2$, initially located at $\mathbf{x}_\gamma(0) = (-20, 0.2)$, sufficiently far upstream of the airfoil, where it essentially convects along the mean-flow direction. In addition, we fix $\eta = 0.8$, which corresponds to a trailing edge flap capturing ten percents of the airfoil chord. The remaining free parameters are therefore the system natural frequency ω and fluid-loading number β, which effects are studied below. The solution for the dynamical problem is obtained numerically using a fourth-order Runge-Kutta algorithm.

To calculate the far-field acoustic radiation, we consider a case where the airfoil is acoustically compact. We therefore assume that $a/\lambda \ll 1$, where $\lambda = 2\pi c_0/\Omega$ is the dimensional acoustic wavelength, with Ω the dimensional counterpart of ω. The condition for airfoil compactness is then given by $a/\lambda = M(\Omega a/2\pi U) \ll 1$, where $M = U/c_0$ is the mean stream Mach number. This restriction is in accordance with the low Mach assumption set for the study of the near-field flow. Making use of Powell-Howe analogy for a compact body [8], and adopting the scaling introduced, we obtain the following form for the *dipole-type* acoustic pressure

$$\frac{p(\mathbf{x},t)}{\rho_0 U^2} = \sqrt{\frac{M}{8|\mathbf{x}|}}\Pi_{\text{tot}}([t]) = \sqrt{\frac{M}{8|\mathbf{x}|}}\left(\Pi_f([t]) + \Pi_\gamma([t]) + \Pi_w([t])\right), \tag{4}$$

where

$$\Pi_f(t_r) \approx \frac{1}{\pi}\cos\alpha\left(\frac{2}{3}\left(1-\eta^2\right)^{3/2} - \eta\left(\pi - \phi_\eta + \frac{\sin 2\phi_\eta}{2}\right)\right)\frac{\partial^2}{\partial t^2}\int_0^{[t]}\frac{\mathrm{d}\theta/\mathrm{d}\tau}{\sqrt{[t]-\tau}}\mathrm{d}\tau, \tag{5}$$

$$\Pi_\gamma(t_r) \approx 2\gamma\left(\sin\alpha\frac{\partial}{\partial t}\int_0^{t_r}\frac{V_\gamma^{(2)}\mathrm{d}\tau}{\sqrt{[t]-\tau}} - \cos\alpha\frac{\partial}{\partial t}\int_0^{t_r}\frac{\left(V_\gamma^{(1)} + \mathrm{i}V_\gamma^{(2)}\right)z_\gamma\mathrm{d}\tau}{\sqrt{(z_\gamma^2-1)([t]-\tau)}}\right), \tag{6}$$

and

$$\Pi_w([t]) \approx \sum_{k=1}^{n} 2\gamma_k\left(\sin\alpha\frac{\partial}{\partial t}\int_0^{[t]}\frac{V_{\gamma_k}^{(2)}\mathrm{d}\tau}{\sqrt{[t]-\tau}} - \cos\alpha\frac{\partial}{\partial t}\int_0^{[t]}\frac{\left(V_{\gamma_k}^{(1)} + \mathrm{i}V_{\gamma_k}^{(2)}\right)z_{\gamma_k}\mathrm{d}\tau}{\sqrt{(z_{\gamma_k}^2-1)([t]-\tau)}}\right), \tag{7}$$

denote the separate contributions of flap motion, incident vortex and wake to the total radiation Π_{tot}, respectively, and t_r marks the scaled retarded time. In (6)-(7), γ_k denotes the strength of the k-th discrete trailing edge vortex according to the Brown and Michael formula, and $V_{\gamma_k}^{(n)}$ and $V_\gamma^{(n)}$ are the velocity components in the n-th direction of the incident and trailing edge vortices, respectively. In addition, z_γ and z_{γ_k} mark the complex-plane locations of incident and k-th trailing-edge vortices, and $\alpha = \cos^{-1}(x_2/|\mathbf{x}|)$ denotes the observer directivity. Note that dipole sound is radiated along both normal ($\propto \cos\alpha$) and mean-flow ($\propto \sin\alpha$) directions, where the latter results directly from vortices motion in the normal direction, reflecting the effect of non-linear vortex-airfoil interactions.

Results and discussion

Figure 2 summarizes some of our results for the dynamical and acoustic problems, by comparing between flap motion and sound radiation in the normal direction for non-flapped airfoil ($\beta = 0$), torsion-free flap ($\beta = 10, \omega = 0$) and flapped airfoil with $\beta = 10, \omega = 1$. Focusing on

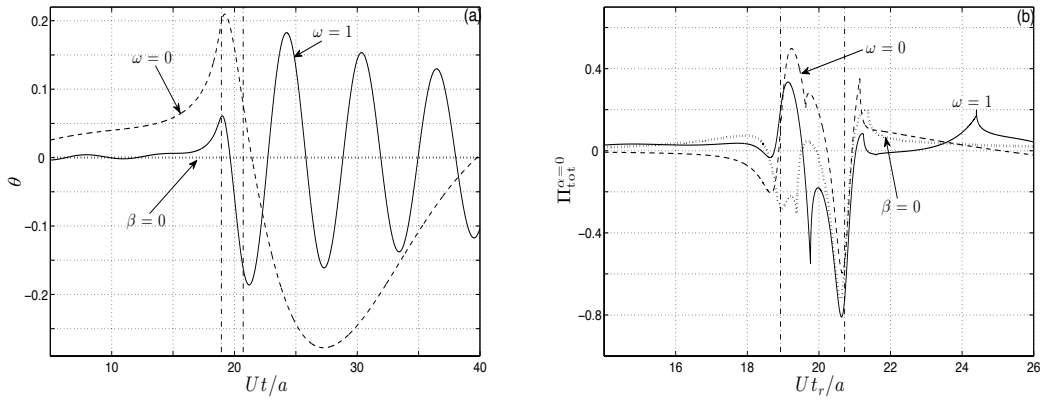

FIGURE 2: Flap angle (Fig. 2a) and total acoustic pressure in the x_2-direction (Fig. 2b) generated by passage of the incident vortex above the airfoil for non-flapped airfoil ($\beta = 0$, dotted lines), torsion-free flap ($\beta = 10$ and $\omega = 0$, dashed lines) and flapped airfoil with $\beta = 10$ and $\omega = 1$ (solid lines). Vertical dash-dotted lines confine the time interval during which the vortex passes above the airfoil.

the latter case (solid line) and examining Fig. 2a, we observe that at early times the incident vortex induces only vanishingly small flap oscillations. Yet, shortly after the incident vortex passes above the airfoil leading edge significant flap oscillations are initiated, characterized by the system natural frequency $\omega = 1$. Remarkably, this frequency is amplified by the fluid-flap system above all other frequencies contained in the spectrum of the forcing vortex. At late times, and as the vortex propagates away from the airfoil, flap oscillations decay. Traversing to the flap motion in the torsion-free $\omega = 0$ case (dashed line in Fig. 2a), we observe qualitatively different behavior: in the absence of a counter-acting spring, the incident vortex freely pulls the flap as it approaches the airfoil (in accordance with the counterclockwise velocity it induces) and pushes it away as it passes above it. This simple “passive-motion" mechanism reduces the singularity of incident vortex interaction with airfoil trailing edge, which, in turn, causes reduction in sound radiation at trailing edge time, as demonstrated below.

The total acoustic radiation along the x_2-direction presented in Fig. 2b can be viewed as a combination of relatively strong leading and trailing edge interactions of the airfoil with the incident vortex, together with late-time sound reflecting the motion of the flap. Interestingly, our results indicate that while flap motion is the indirect cause for late-time radiation, direct flap sound (Π_f) is always negligible, and the acoustic radiation is dominated by incident and trailing edge wake sound at all times. Examining the flap-on-spring (solid), torsion-free (dashed) and non-flapped (dotted) signatures, we find that at trailing edge time (i.e., when the incident vortex passes above airfoil trailing edge, which is typically the time when strongest sound is radiated), the flap may have an amplifying (for $\omega = 1$) or absorbing (for $\omega = 0$) effect on radiation compared with the rigid case (cf. the levels of sound in the vicinity of the vertical right line in Fig. 2b). This result is in accordance with the “passive-motion" mechanism described in Fig. 2a for the $\omega = 0$ case.

To clarify the effect of ω on system acoustic signature, Fig. 3a presents the far-field sound energy amplitude,

$$\mathscr{P}_{\rm tot}(t_r) = \int_0^{2\pi} \Pi^2_{\rm tot}(t_r, \alpha)\,\mathrm{d}\alpha, \tag{8}$$

obtained by quadrature of the squared total acoustic pressure (4) over a circle of radius $|\mathbf{x}| \to \infty$. The solid line shows the acoustic amplitude for a non-flapped airfoil ($\beta = 0$), and the dashed and dash-dotted lines present the counterpart results for $\beta = 10$ with $\omega = 0$ and $\omega = 1$, respectively. As noted in Fig. 2b, we observe that the largest sound energy amplitude is obtained in the

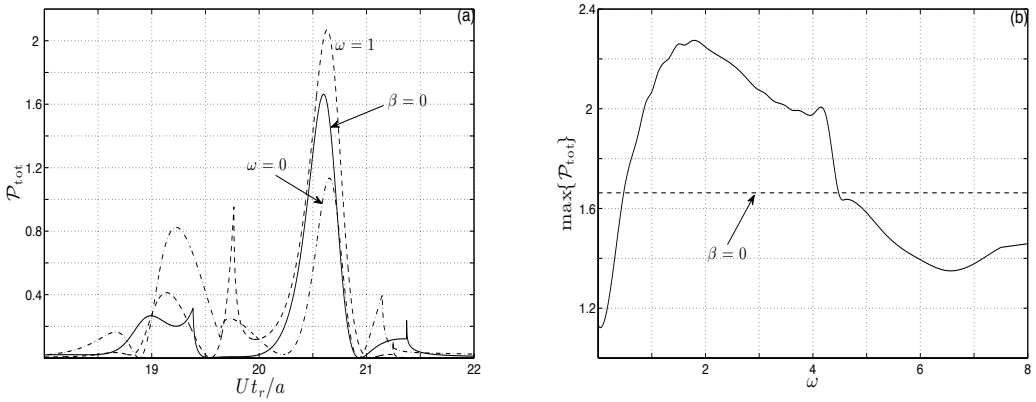

FIGURE 3: Effect of system natural frequency on sound energy amplitude $\mathscr{P}_{\rm tot}$: (a) comparison between $\mathscr{P}_{\rm tot}$ for different flap configurations (line types as in Fig. 2); (b) variation of maximum $\mathscr{P}_{\rm tot}$ with ω, achieved at trailing edge time.

proximity of trailing edge time (at $Ut_r/a \approx 20.7$), and thus focus on the effect of ω at that time. This effect is illustrated in Fig. 3b, where the maximum value of $\mathscr{P}_{\rm tot}$ is shown as function of ω. For reference, the counterpart sound energy amplitude in the case of a rigid airfoil (i.e., the maximum value of the solid line in Fig. 3a) is given by the dashed line. In support of Fig. 2b, the results confirm that the flap may act as sound "amplifier" or "absorber", depending on the value of system natural frequency: at $0.5 < \omega < 4.5$, the flap amplifies sound energy amplitude above the reference rigid-airfoil value, while at lower and larger frequencies the flap attenuates radiation. Note that at large values of ω (not presented here), $\mathscr{P}_{\rm tot}$ converges to its non-flapped form, as flap oscillations vanish and the airfoil becomes essentially rigid. Further results rationalizing the above findings will be discussed elsewhere [9].

ACKNOWLEDGMENTS

A.M. acknowledges support by the Marie Curie International Reintegration Grant No. PIRG-GA-2010-276837. L.H. acknowledges the support of a China National Key Basic Research Scheme project No. 2012CB720202.

REFERENCES

[1] M.J.T. Smith, *Aircraft Noise*, (Cambridge University Press, Cambridge,1989), 382 pp.

[2] M.S. Howe, "On the generation of side-edge flap noise," Journal of Sound and Vibration **80**, 555-572 (1982).

[3] Y.P. Guo, "A Discrete Vortex Model for Slat Noise Prediction," AIAA Paper 2001-2157 (2001).

[4] Z.C. Zheng, B.K. Tan and Y. Xu, "Near-field fluctuations and far-field noise of a three-element airfoil system by a discrete vortex method," Applied Mathematics and Computation **216**, 1072-1086 (2010).

[5] F.V. Hutcheson, T.F. Brooks and W.M. Humphreys, "Noise radiation from a continuous mold-line link flap configuration," International Journal of Aeroacoustics **10**, 565-588 (2011).

[6] C.E. Brown and W.H. Michael, "Effect of leading edge separation on the lift of a delta wing," Journal of the Aeronautical Sciences **21**, 690-706 (1954).

[7] M.S. Howe, “Emendation of the Brown & Michael equation, with application to sound generation by vortex motion near a half-plane," Journal of Fluid Mechanics **329**, 89-101 (1996).

[8] M.S. Howe, *Theory of Vortex Sound* (Cambridge University Press, Cambridge, 2003), 216 pp.

[9] A. Manela and L. Huang, “Point vortex model for prediction of sound generated by a wing with flap interacting with a passing vortex," Journal of the Acoustical Society of America, submitted (2012).